HO CHI MINH CITY UNIVERSITY OF TECHNOLOGY
AND EDUCATION
FALCUTY OF MECHANICAL ENGINEERING
DEPARTMENT OF MECHATRONICS

REPORT AND SIMULATION OF A 6 DOF ROBOT

COURSE CODE:	MOCO331929E_23_2_01	
Teacher:	Tran Minh Thien	
Member:	Nguyen Trinh Tra Giang	22134005
	Vo Hong Quan	22314012

Table of Contents

INTRODUCTION

In an era where technological advancements are pivotal to industrial, military, and security breakthroughs, robots emerge as critical players. The realm of robotics is evolving at an unprecedented rate, permeating diverse sectors with its transformative potential. Among the myriad robotic systems revolutionizing these fields, the six-degree-of-freedom (6-DOF) robot stands out as a paragon of versatility and efficiency. These robots are renowned for their dexterity and precision, which render them indispensable for tasks ranging from intricate assembly to complex surgical procedures.

As we endeavor to optimize these mechanical marvels for enhanced performance and energy conservation, the study of kinematic motion becomes indispensable. Kinematics—the branch of mechanics concerned with the motion of objects without reference to the forces that cause the motion—serves as the foundation for robot movement and control. This encompasses a spectrum of calculations such as forward and inverse kinematics, velocity kinematics, and static force analysis. Through rigorous simulation and kinematic computation, we can garner critical insights into the operational nuances of robots.

This report delves into the methodologies for kinematic calculation, employing both theoretical and simulation-based approaches to dissect the functionalities of a 6-DOF robot. Our objective is to not only augment the performance and energy efficiency of these robots but also to expand our comprehension of their capabilities and applications. By dissecting the mechanics of motion and control, we aim to contribute to the field of robotics, enhancing the synergy between mechanical sophistication and operational efficacy.

I. OVERVIEW

1. Introduction to industrial robots

Industrial robots have not only transformed manufacturing processes but also redefined the nature of work itself. Their integration into production lines has led to significant improvements in efficiency, consistency, and safety. One of the most notable impacts of industrial robots is their ability to handle tasks that are repetitive, dangerous, or require extreme precision, thereby reducing the risk of accidents and injuries for human workers.

Furthermore, the evolution of industrial robots has led to the development of collaborative robots, or cobots, designed to work alongside humans in shared workspaces. These cobots are equipped with advanced sensors and safety features that allow them to interact safely with human operators, opening up new possibilities for human-robot collaboration and flexible manufacturing systems.

Moreover, the advent of artificial intelligence (AI) and machine learning has enabled industrial robots to become more adaptable and autonomous. These intelligent robots can learn from experience, optimize their performance, and even anticipate changes in the production environment, further enhancing productivity and efficiency.

In addition to their role in traditional manufacturing sectors, industrial robots are also making significant strides in emerging industries such as healthcare, logistics, and agriculture. From assisting surgeons in delicate procedures to autonomously harvesting crops in fields, industrial robots are expanding their applications and reshaping various aspects of society.

Looking ahead, the continued advancement of industrial robotics technology holds the promise of even greater innovation and disruption. As robots become increasingly sophisticated, versatile, and affordable, they will continue to play a vital role in driving economic growth, competitiveness, and sustainability in the global manufacturing landscape. With ongoing research and development efforts, industrial robots are poised to usher in a new era of automation, efficiency, and prosperity for industries and societies worldwide.

In the year 2022, an estimated 3,903,633 industrial robots were in operation worldwide according to International Federation of Robotics (IFR).

2. Introduction to ABB Corporation

ABB Corporation's journey over the decades highlights its pivotal role in shaping global industrial automation and power technology landscapes. From its inception, ABB has been at the forefront of technological innovation, continually expanding its offerings to meet the changing demands of the global market.

Throughout the 2000s, ABB's strategic divestitures and acquisitions focused on streamlining its operations and enhancing its core competencies in robotics, automation, and energy management. This period saw significant advancements in its product lines, introducing more energy-efficient systems and solutions that catered to a growing global emphasis on sustainable practices. ABB's commitment to sustainability is evident in its development of products like high-efficiency motors and drives, which not only reduce energy consumption but also decrease operational costs for businesses.

In recent years, ABB has continued to innovate, particularly in the realms of digitalization and smart technologies. The introduction of the ABB Ability™ platform showcases its commitment to the future of industry 4.0, offering scalable digital solutions that enable customers to enhance performance and productivity while minimizing environmental impact. This platform integrates IoT, artificial intelligence, and analytics to provide actionable insights that drive efficiency and optimize industrial operations.

Moreover, ABB's influence extends beyond traditional industrial sectors. Its ventures into electric vehicle infrastructure demonstrate an adaptive approach to market needs, reflecting the shift towards renewable energy sources. The company's involvement in building the infrastructure for electric vehicles, such as high-speed charging stations, positions ABB as a key player in supporting the transition to a more sustainable transportation sector.

Looking towards the future, ABB is poised to lead the way in pioneering technologies that will further revolutionize industries. The integration of AI and machine learning into its offerings will likely enhance its product lines, making industrial processes more adaptive and intelligent. As global industries evolve towards more integrated and environmentally friendly practices, ABB's role in facilitating this transition will undoubtedly be critical, reinforcing its status as a leader in global industrial innovation and sustainable development.

3. Robot IRB 6700

3.1 Introduction

The IRB 6700 series represents ABB Robotics' 7th generation of industrial robots, offering high payload capacity and exceptional performance. Building upon the success of the renowned IRB 6640 series, the IRB 6700 robots feature a large working range, robust wrist torque, modular design for ease of service, and the reliability that ABB's robots are known for.

What sets the IRB 6700 family apart is its emphasis on high production capacity, compact design, and low weight, making it ideal for a wide range of process applications across various industries. These robots are engineered to deliver superior performance while minimizing downtime, servicing complexity, and maintenance costs.

Whether it's handling heavy payloads, executing precise assembly tasks, or operating in challenging environments, the IRB 6700 series excels in delivering consistent and reliable performance. Its versatility and efficiency make it a preferred choice for manufacturers seeking to optimize their production processes and achieve higher levels of productivity.

In summary, the IRB 6700 series embodies ABB Robotics' commitment to innovation, quality, and customer satisfaction. With its advanced features, robust construction, and industry-leading performance, these robots are poised to meet the evolving needs of modern manufacturing and drive efficiency and competitiveness for businesses worldwide.

3.2 Abilities of IRB 6700

- Strength and Versatility: robot brings strength and versatility to the production line, stronger than previous models and aids in reducing manufacturing costs.
- Maintenance Cost Reduction: helps decrease maintenance costs over its lifespan. Simplified maintenance routines contribute to increased uptime during production.
- Enhanced Uptimes: boasts longer uptimes compared to previous models. Minimum time between failures is reported to be 400,000 hours.
- Power Consumption Reduction: The robot reduces power consumption by 15%, leading to cost savings for companies.
- Serviceability Improvement: improved serviceability, enhancing its overall performance.
- Precision and Accuracy: The robot excels in performing with precision, capable of executing tasks with pinpoint accuracy. It can move parts along a belt sander with precision, reducing errors significantly.
- Application Speed Increase: Companies can experience up to a 5% increase in application speed with the IRB 6700.

3.3 Applications

The ABB IRB 6700-150/3.20 robot is a versatile industrial robot with a wide range of applications. Some common applications of this robot model include:

- Additive Manufacturing: The IRB 6700-150/3.20 can be used in additive manufacturing processes, such as 3D printing, to build complex components layer by layer.
- Assembly: This robot is well-suited for assembly tasks, where it can precisely manipulate and assemble components with high accuracy and repeatability.
- Dispensing: The IRB 6700-150/3.20 can be employed in dispensing applications, such as applying adhesives, sealants, or coatings, with controlled and consistent dispensing patterns.
- Finishing: In finishing applications, the robot can perform tasks such as polishing, deburring, or grinding to achieve smooth and uniform surfaces on workpieces.
- Material Handling: Material handling is one of the primary applications of the IRB 6700-150/3.20, where it can efficiently transport, stack, palletize, or de-palletize materials in manufacturing facilities.
- Palletizing: The robot can automate palletizing tasks, stacking products or materials onto pallets in a predefined pattern for storage or transportation.
- Remote TCP: The IRB 6700-150/3.20 supports Remote TCP (Tool Center Point), allowing the robot's end-effector to be controlled and adjusted remotely, enabling precise positioning and alignment of tools or workpieces.

3.4 Technical specifications of IRB 6700 150/320

a. Mechanical structure

- Manipulation weight: 1280(kg)
- Handling capacity (kg): 150
- Reach (m): 3.20
- Robot axes:

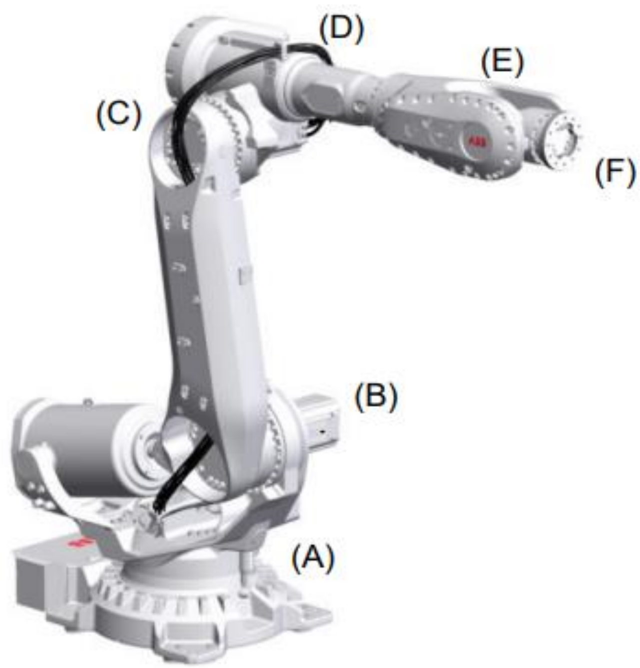

Pos	Description	Pos	Description
A	Axis 1	B	Axis 2
C	Axis 3	D	Axis 4
E	Axis 5	F	Axis 6

- Main dimensions of IRB 6700 150/320:

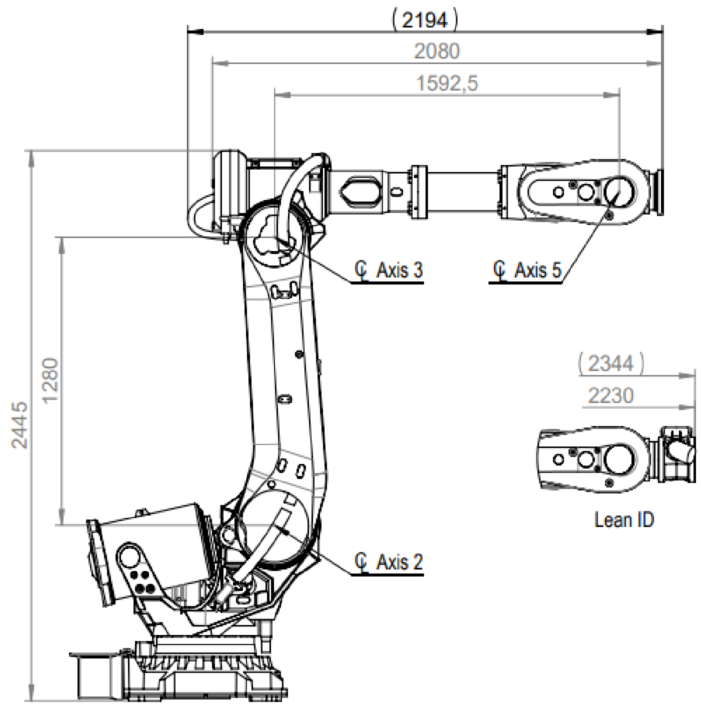

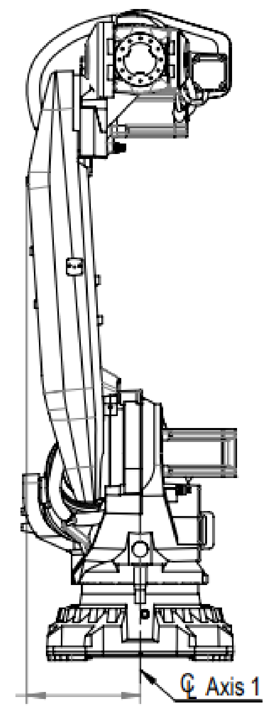

-

Front view

Right side view

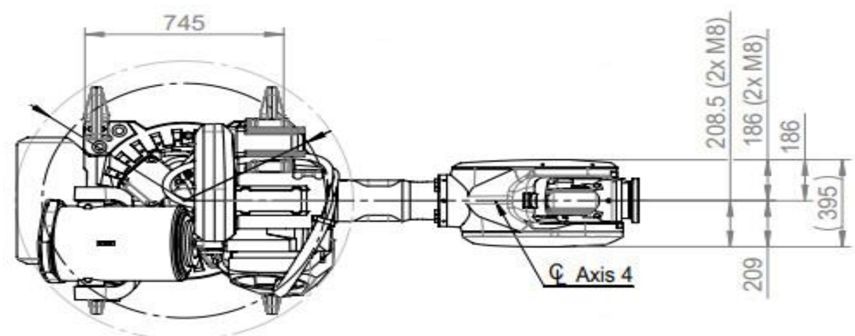

Top view

b. <u>Standard</u>

- Normative standards as referred to from ISO 10218-1:

Standard	**Description**
ISO 9283:1998	Manipulating industrial robots - Performance criteria and related test methods
ISO 10218-2	Manipulating industrial robots - Performance criteria and related test methods
ISO 12100	Safety of machinery - General principles for design - Risk assessment and risk reduction
ISO 13849-1:2006	Safety of machinery - Safety related parts of control systems - Part 1: General principles for design
ISO 13850	Safety of machinery - Emergency stop - Principles for design
IEC 60204-1	Safety of machinery - Electrical equipment of machines - Part 1: General requirements

- Region specific standards and regulations:

Standard	Description
ANSI/RIA R15.06	Safety requirements for industrial robots and robot systems
ANSI/UL 1740	Safety standard for robots and robotic equipment
CAN/CSA Z 434-03	Industrial robots and robot Systems - General safety requirements

c. <u>Installation</u>

- Protection standards:

Robot variant/Protection standard	IEC 60529
All variants, manipulator	IP67

- Explosive environments: The robot must not be located or operated in an explosive environment.
- Ambient temperature:

Description	**Standard/Option**	**Temperature**
Manipulator during operation	Standard	Minimum: +5°Ci (41°F) Maximum: +50°C (122°F)
For the controller	Standard/Option	See Product specification - Controller IRC5
Complete robot during transportation and storage	Standard	Minimum: -25°C (-13°F) Maximum: +55°C (+131°F)
For short periods (not exceeding 24 hours)	Standard	+70°C (+158°F)

- Relative humidity:

Description	**Relative humidity**
Complete robot during transportation and storage	Maximum 95% at constant temperature.
Complete robot during operation	Maximum 95% at constant temperature.

d. Robot motion

- Type of motion:

Axis	**Type of motion**	**Range of movement - IRB 6700**
Axis1	Rotation motion	±170° or ±220°(option)
Axis 2	Arm motion	-65°/+85°
Axis 3	Arm motion	-180°/+70°
Axis 4	Wrist motion	±300°
Axis 5	Bend motion	±130°
Axis 6	Turn motion	±93.7 revolutions

- Working range:

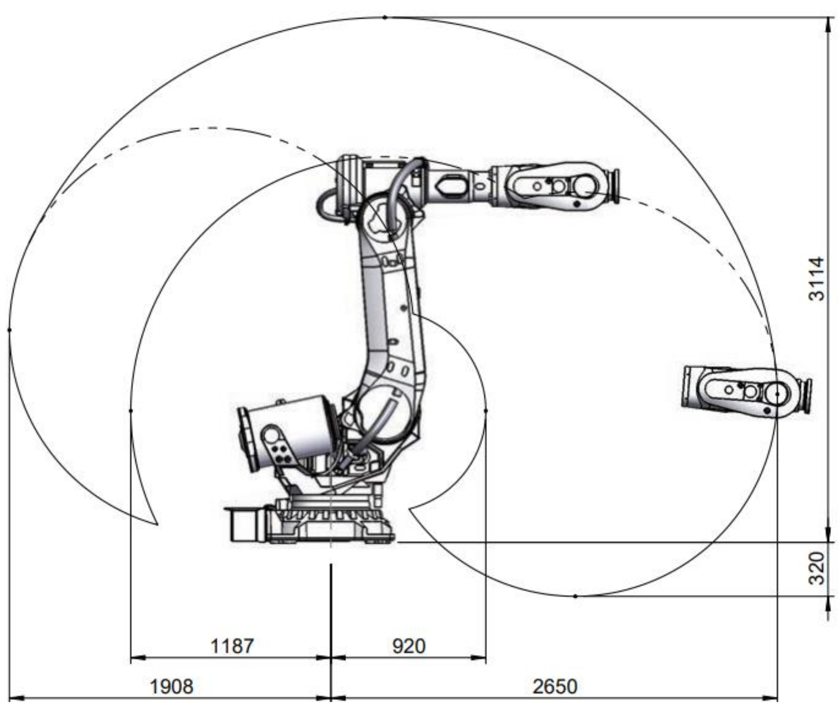

- Performance according to ISO 9283:

IRB 6700 150/3.20	
Pose accuracy, AP (mm)	0.05
Pose repeatability, RP (mm)	0.06
Pose stabilization time, PSt (s) within 0.5 mm of the position	0.34
Path accuracy, AT (mm)	1.6
Path repeatability, RT (mm)	0.14

- Maximum axis speed:

Axis 1	**Axis 2**	**Axis 3**	**Axis 4**	**Axis 5**	**Axis 6**
100 °/s	90 °/s	90 °/s	170 °/s	120 °/s	190 °/s

II. CALCULATION OF KINEMATIC MOTION

1. Determine rotation matrix

We have rotation matrix: ${}^{G}R_B = \begin{bmatrix} r_{11} & r_{12} & r_{13} \\ r_{21} & r_{22} & r_{23} \\ r_{31} & r_{32} & r_{33} \end{bmatrix}$

A translation matrix: ${}^{G}d = \begin{bmatrix} X_0 \\ Y_0 \\ Z_0 \end{bmatrix}$

And we expand both to a 4x4 matrix:

$$
{}^{G}R_B = \begin{bmatrix} r_{11} & r_{12} & r_{13} & 0 \\ r_{21} & r_{22} & r_{23} & 0 \\ r_{31} & r_{32} & r_{33} & 0 \\ 0 & 0 & 0 & 1 \end{bmatrix}, \ {}^{G}d = \begin{bmatrix} 1 & 0 & 0 & X_0 \\ 0 & 1 & 0 & Y_0 \\ 0 & 0 & 1 & Z_0 \\ 0 & 0 & 0 & 1 \end{bmatrix}
$$

By multiplication of two matrix above, homogenous transformation matrix ${}^{G}T_B$ can be described as:

$$
{}^{G}T_B = {}^{G}D_B\,{}^{G}R_B = \begin{bmatrix} 1 & 0 & 0 & X_0 \\ 0 & 1 & 0 & Y_0 \\ 0 & 0 & 1 & Z_0 \\ 0 & 0 & 0 & 1 \end{bmatrix} \begin{bmatrix} r_{11} & r_{12} & r_{13} & 0 \\ r_{21} & r_{22} & r_{23} & 0 \\ r_{31} & r_{32} & r_{33} & 0 \\ 0 & 0 & 0 & 1 \end{bmatrix} = \begin{bmatrix} r_{11} & r_{12} & r_{13} & X_0 \\ r_{21} & r_{22} & r_{23} & Y_0 \\ r_{31} & r_{32} & r_{33} & Z_0 \\ 0 & 0 & 0 & 1 \end{bmatrix}
$$

We will first demonstrate how to calculate a position of any point when it is rotated and translated before going into our robot kinematics solution through example below.

Example:

Point A, with local coordinates ${}^{B}r = \begin{bmatrix}100 & 200 & 300\end{bmatrix}^T (mm)$, rotates by $\alpha = \frac{\pi}{6}$ (rad) about X-axis and translates to $\begin{bmatrix}30 & 50 & 70\end{bmatrix}^T (mm)$. Find the global position of point?

Solve:

Substitute $\alpha = \frac{\pi}{6}$ (rad), $X_0 = 30$ (mm), $Y_0 = 50$ (mm), $Z_0 = 70$ (mm) into the homogenous transformation matrix:

$${}^{G}T_B = {}^{G}D_B \, {}^{G}R_B$$

$$= \begin{bmatrix} 1 & 0 & 0 & 30 \\ 0 & cos\left(\frac{\pi}{6}\right) & -sin\left(\frac{\pi}{6}\right) & 50 \\ 0 & sin\left(\frac{\pi}{6}\right) & cos\left(\frac{\pi}{6}\right) & 70 \\ 0 & 0 & 0 & 1 \end{bmatrix}$$

Where as: ${}^{G}R_B = \begin{bmatrix} 1 & 0 & 0 & 0 \\ 0 & cos(\alpha) & -sin(\alpha) & 0 \\ 0 & sin(\alpha) & cos(\alpha) & 0 \\ 0 & 0 & 0 & 1 \end{bmatrix}$, ${}^{G}D_B = \begin{bmatrix} 1 & 0 & 0 & X_0 \\ 0 & 1 & 0 & Y_0 \\ 0 & 0 & 1 & Z_0 \\ 0 & 0 & 0 & 1 \end{bmatrix}$

Location of A in global coordinates:

$${}^{G}r_B = {}^{G}T_B \, {}^{B}r$$

$$= \begin{bmatrix} 1 & 0 & 0 & 30 \\ 0 & cos\left(\frac{\pi}{6}\right) & -sin\left(\frac{\pi}{6}\right) & 50 \\ 0 & sin\left(\frac{\pi}{6}\right) & cos\left(\frac{\pi}{6}\right) & 70 \\ 0 & 0 & 0 & 1 \end{bmatrix} \begin{bmatrix} 100 \\ 200 \\ 300 \\ 1 \end{bmatrix} = \begin{bmatrix} 60 \\ 58.301 \\ 155.62 \\ 1 \end{bmatrix} (\text{mm})$$

2. Forward kinematic

2.1 D-H table

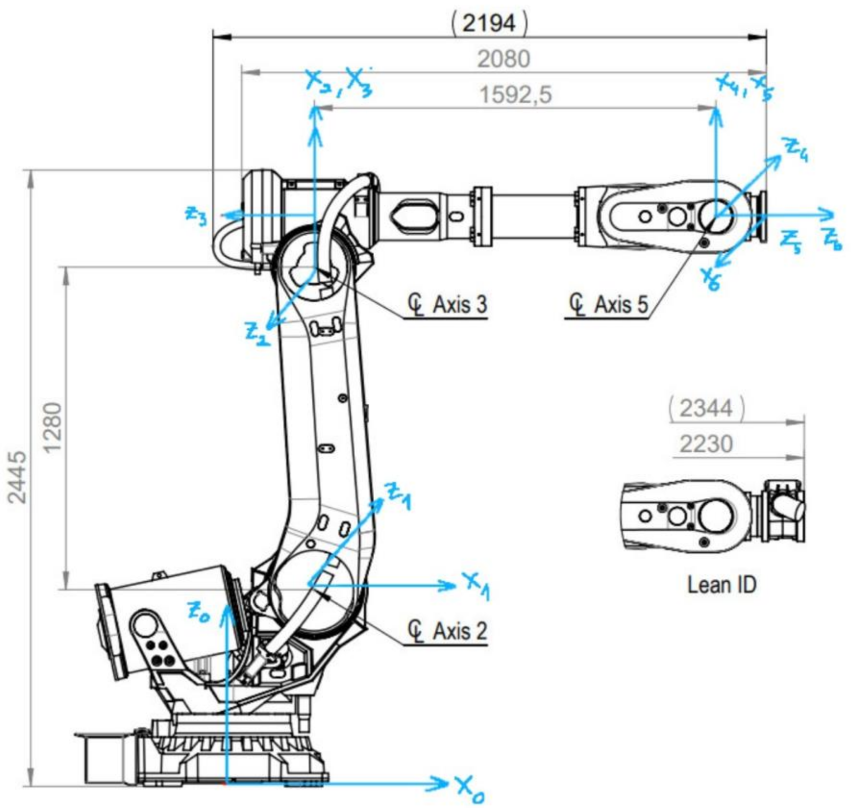

(Unit: mm)

Link	a_i (mm)	α_i (rad)	d_i (mm)	θ_i (rad)	
1	320	$\frac{\pi}{2}$	780	θ_1	$R \vdash R\left(\frac{\pi}{2}\right)$
2	1280	π	0	θ_2	$R \parallel R(\pi)$
3	200	$\frac{\pi}{2}$	0	θ_3	$R \vdash R\left(\frac{\pi}{2}\right)$
4	0	$\frac{\pi}{2}$	-1595.5	θ_4	$R \vdash R\left(\frac{\pi}{2}\right)$
5	0	$\frac{\pi}{2}$	0	θ_5	$R \vdash R\left(\frac{\pi}{2}\right)$
6	0	0	200	θ_6	$R \parallel R(0)$

2.2 Components of rotation matrix

- Transformation matrix between robot links:

$$^{i-1}T_i = D_{z_{i-1},d_i} R_{z_{i-1},\theta_i} D_{x_{i-1},a_i} R_{x_{i-1},\alpha_i}$$

$$= \begin{bmatrix} cos\theta_i & -sin\theta_i cos\alpha_i & sin\theta_i sin\alpha_i & a_i cos\theta_i \\ sin\theta_i & cos\theta_i cos\alpha_i & -cos\theta_i sin\alpha_i & a_i sin\theta_i \\ 0 & sin\alpha_i & cos\alpha_i & d_i \\ 0 & 0 & 0 & 1 \end{bmatrix}$$

Where:

$$D_{z_{i-1},d_i} = \begin{bmatrix} 1 & 0 & 0 & 0 \\ 0 & 1 & 0 & 0 \\ 0 & 0 & 1 & d_i \\ 0 & 0 & 0 & 1 \end{bmatrix} \qquad R_{z_{i-1},\theta_i} = \begin{bmatrix} cos\,\theta_i & -sin\,\theta_i & 0 & 0 \\ sin\,\theta_i & cos\,\theta_i & 0 & 0 \\ 0 & 0 & 1 & 0 \\ 0 & 0 & 0 & 1 \end{bmatrix}$$

$$D_{x_{i-1},a_i} = \begin{bmatrix} 1 & 0 & 0 & a_i \\ 0 & 1 & 0 & 0 \\ 0 & 0 & 1 & 0 \\ 0 & 0 & 0 & 1 \end{bmatrix} \qquad R_{x_{i-1},\alpha_i} = \begin{bmatrix} 1 & 0 & 0 & 0 \\ 0 & cos\,\alpha_i & -sin\,\alpha_i & 0 \\ 0 & sin\,\alpha_i & cos\,\alpha_i & 0 \\ 0 & 0 & 0 & 1 \end{bmatrix}$$

- From DH table's values, we can deduce that:

- Link 1: $\theta_1 \in [-170°,170°] \rightarrow \left[\frac{-17}{18}\pi(rad), \frac{17}{18}\pi(rad)\right]$

$$^0T_1 = \begin{bmatrix} cos\,\theta_1 & 0 & sin\,\theta_1 & 320\,cos\,\theta_1 \\ sin\,\theta_1 & 0 & -cos\,\theta_1 & 320\,sin\,\theta_1 \\ 0 & 1 & 0 & 780 \\ 0 & 0 & 0 & 1 \end{bmatrix}$$

- Link 2: $\theta_2 \in [5°,155°] \rightarrow \left[\frac{1}{36}\pi(rad), \frac{31}{36}\pi(rad)\right]$

$$^{1}T_2 = \begin{bmatrix} \cos\theta_2 & \sin\theta_2 & 0 & 1280\cos\theta_2 \\ \sin\theta_2 & -\cos\theta_2 & 0 & 1280\sin\theta_2 \\ 0 & 0 & -1 & 0 \\ 0 & 0 & 0 & 1 \end{bmatrix}$$

- Link 3: $\theta_3 \in [-180°,70°] \rightarrow \left[-\pi(rad), \frac{7}{18}\pi(rad)\right]$

$$^{2}T_3 = \begin{bmatrix} \cos\theta_3 & 0 & \sin\theta_3 & 200\cos\theta_3 \\ \sin\theta_3 & 0 & -\cos\theta_3 & 200\sin\theta_3 \\ 0 & 1 & 0 & 0 \\ 0 & 0 & 0 & 1 \end{bmatrix}$$

- Link 4: $\theta_4 \in [-300°,300°] \rightarrow \left[-\frac{5}{3}\pi(rad), \frac{5}{3}\pi(rad)\right]$

$$^{3}T_4 = \begin{bmatrix} \cos\theta_4 & 0 & \sin\theta_4 & 0 \\ \sin\theta_4 & 0 & -\cos\theta_4 & 0 \\ 0 & 1 & 0 & -1592.5 \\ 0 & 0 & 0 & 1 \end{bmatrix}$$

- Link 5: $\theta_5 \in [-130°,130°] \rightarrow \left[-\frac{13}{18}\pi(rad), \frac{13}{18}\pi(rad)\right]$

$$^{4}T_5 = \begin{bmatrix} \cos\theta_5 & 0 & \sin\theta_5 & 0 \\ \sin\theta_5 & 0 & -\cos\theta_5 & 0 \\ 0 & 1 & 0 & 0 \\ 0 & 0 & 0 & 1 \end{bmatrix}$$

- Link 6: $\theta_6 \in [-360°, 360°] \rightarrow [-2\pi(rad), 2\pi(rad)]$

$$ {}^{5}T_6 = \begin{bmatrix} cos\theta_6 & -sin\theta_6 & 0 & 0 \\ sin\theta_6 & cos\theta_6 & 0 & 0 \\ 0 & 0 & 1 & 200 \\ 0 & 0 & 0 & 1 \end{bmatrix} $$

- From these transformation matrices, we can conclude that the transformation matrix to convert position from the end working point to the global coordinate origin is:

$$ {}^{0}T_6 = {}^{0}T_1\,{}^{1}T_2\,{}^{2}T_3\,{}^{3}T_4\,{}^{4}T_5\,{}^{5}T_6 = \begin{bmatrix} r_{11} & r_{12} & r_{13} & r_{14} \\ r_{21} & r_{22} & r_{23} & r_{24} \\ r_{31} & r_{32} & r_{33} & r_{34} \\ 0 & 0 & 0 & 1 \end{bmatrix} $$

Where:

$$ r_{11} = s\theta_6\left[c\theta_4 s\theta_1 + s\theta_4\left(c\theta_1 s\theta_2 s\theta_3 + c\theta_1 c\theta_2 c\theta_3\right)\right] $$
$$ -c\theta_6\left\{c\theta_5\left[s\theta_1 s\theta_4 - c\theta_4\left(c\theta_1 s\theta_2 s\theta_3 + c\theta_1 c\theta_2 c\theta_3\right)\right] - s\theta_5\left(c\theta_1 c\theta_2 s\theta_3 - c\theta_1 c\theta_2 s\theta_2\right)\right\} $$

$$ r_{12} = c\theta_6\left[c\theta_4 s\theta_1 + s\theta_4\left(c\theta_1 s\theta_2 s\theta_3 + c\theta_1 c\theta_2 c\theta_3\right)\right] $$
$$ + s\theta_6\left\{c\theta_5\left[s\theta_1 s\theta_4 - c\theta_4\left(c\theta_1 s\theta_2 s\theta_3 + c\theta_1 c\theta_2 c\theta_3\right)\right] - s\theta_5\left(c\theta_1 c\theta_2 s\theta_3 - c\theta_1 c\theta_3 s\theta_2\right)\right\} $$

$$ r_{13} = -s\theta_5\left[s\theta_1 s\theta_4 - c\theta_4\left(c\theta_1 s\theta_2 s\theta_3 + c\theta_1 c\theta_2 c\theta_3\right)\right] - c\theta_5\left(c\theta_1 c\theta_2 s\theta_3 - c\theta_1 c\theta_3 s\theta_2\right) $$

$$ r_{14} = 320c\theta_1 + 1280c\theta_1 c\theta_2 + 200c\theta_1 s\theta_2 s\theta_3 - 200s\theta_1 s\theta_4 s\theta_5 $$
$$ + 200s\left(\theta_2 - \theta_3\right)c\theta_1 c\theta_5 + 200c\theta_1 c\theta_2 c\theta_3 - \frac{3185c\theta_1 c\theta_2 s\theta_3}{2} $$
$$ + \frac{3185c\theta_1 c\theta_3 s\theta_2}{2} + 200c\theta_1 c\theta_2 c\theta_3 c\theta_4 s\theta_5 + 200c\theta_1 c\theta_4 s\theta_2 s\theta_3 s\theta_5 $$

$$ r_{21} = c\theta_6\left\{c\theta_5\left[c\theta_1 s\theta_4 + c\theta_4\left(s\theta_1 s\theta_2 s\theta_3 + c\theta_2 c\theta_3 s\theta_1\right)\right] + s\theta_5\left(c\theta_2 s\theta_1 s\theta_3 - c\theta_3 s\theta_1 s\theta_2\right)\right\} $$
$$ - s\theta_6\left[c\theta_1 c\theta_4 - s\theta_4\left(s\theta_1 s\theta_2 s\theta_3 + c\theta_2 c\theta_3 s\theta_1\right)\right] $$

$$r_{22} = -c\theta_6\left[c\theta_1 c\theta_4 - s\theta_4\left(s\theta_1 s\theta_2 s\theta_3 + c\theta_2 c\theta_3 s\theta_1\right)\right]$$
$$-s\theta_6\left\{c\theta_5\left[c\theta_1 s\theta_4 + c\theta_4\left(s\theta_1 s\theta_2 s\theta_3 + c\theta_2 c\theta_3 s\theta_1\right)\right] + s\theta_5\left(c\theta_2 s\theta_1 s\theta_3 - c\theta_3 s\theta_1 s\theta_2\right)\right\}$$

$$r_{23} = s\theta_5\left[c\theta_1 s\theta_4 + c\theta_4\left(s\theta_1 s\theta_2 s\theta_3 + c\theta_2 c\theta_3 s\theta_1\right)\right] - c\theta_5\left(c\theta_2 s\theta_1 s\theta_3 - c\theta_3 s\theta_1 s\theta_2\right)$$

$$r_{24} = 320s\theta_1 + 1280c\theta_2 s\theta_1 - \frac{3185c\theta_2 s\theta_1 s\theta_3}{2} + \frac{3185c\theta_3 s\theta_1 s\theta_2}{2} + 200c\theta_1 s\theta_4 s\theta_5$$
$$+200s\theta_1 s\theta_2 s\theta_3 + 200s\left(\theta_2 - \theta_3\right)c\theta_5 s\theta_1 + 200c\theta_2 c\theta_3 s\theta_1 + 200c\theta_2 c\theta_3 c\theta_4 s\theta_1 s\theta_5$$
$$+200c\theta_4 s\theta_1 s\theta_2 s\theta_3 s\theta_5$$

$$r_{31} = c\theta_6\left[c\left(\theta_2 - \theta_3\right)s\theta_5 + s\left(\theta_2 - \theta_3\right)c\theta_4 c\theta_5\right] + s\left(\theta_2 - \theta_3\right)s\theta_4 s\theta_6$$

$$r_{32} = s\left(\theta_2 - \theta_3\right)c\theta_6 s\theta_4 - s\theta_6\left[c\left(\theta_2 - \theta_3\right)s\theta_5 + s\left(\theta_2 - \theta_3\right)c\theta_4 c\theta_5\right]$$

$$r_{33} = s\left(\theta_2 - \theta_3\right)c\theta_4 s\theta_5 - c\left(\theta_2 - \theta_3\right)c\theta_5$$

$$r_{34} = 200s\left(\theta_2 - \theta_3\right) - \frac{3185c\left(\theta_2 - \theta_3\right)}{2} + 1280s\theta_2 + 100s\left(\theta_2 - \theta_3\right)s\left(\theta_4 + \theta_5\right)$$
$$-200c\left(\theta_2 - \theta_3\right)c\theta_5 - 100s\left(\theta_2 - \theta_3\right)s\left(\theta_4 - \theta_5\right) + 780$$

With: $s\theta_i = sin(\theta_i)$, $c\theta_i = cos(\theta_i)$

2.3 Example

Let $\theta_1 = -\frac{\pi}{4}, \theta_2 = \frac{13}{18}\pi, \theta_3 = \frac{2}{9}\pi, \theta_4 = 0, \theta_5 = -\frac{\pi}{2}, \theta_6 = 0$ (All angles are in radian). Find the global position of the point P = $\begin{bmatrix} P_x & P_y & P_z \end{bmatrix}^T$ (mm)

Substitute all the angles, we get the following homogenous transformation matrices:

$$^0T_1 = \begin{bmatrix} cos\left(-\frac{\pi}{4}\right) & 0 & sin\left(-\frac{\pi}{4}\right) & 320\,cos\left(-\frac{\pi}{4}\right) \\ sin\left(-\frac{\pi}{4}\right) & 0 & -cos\left(-\frac{\pi}{4}\right) & 320\,sin\left(-\frac{\pi}{4}\right) \\ 0 & 1 & 0 & 780 \\ 0 & 0 & 0 & 1 \end{bmatrix}$$

$$^1T_2 = \begin{bmatrix} cos\left(\frac{13}{18}\pi\right) & sin\left(\frac{13}{18}\pi\right) & 0 & 1280\,cos\left(\frac{13}{18}\pi\right) \\ sin\left(\frac{13}{18}\pi\right) & -cos\left(\frac{13}{18}\pi\right) & 0 & 1280\,sin\left(\frac{13}{18}\pi\right) \\ 0 & 0 & -1 & 0 \\ 0 & 0 & 0 & 1 \end{bmatrix}$$

$$^2T_3 = \begin{bmatrix} cos\left(\frac{2}{9}\pi\right) & 0 & sin\left(\frac{2}{9}\pi\right) & 200\,cos\left(\frac{2}{9}\pi\right) \\ sin\left(\frac{2}{9}\pi\right) & 0 & -cos\left(\frac{2}{9}\pi\right) & 200\,sin\left(\frac{2}{9}\pi\right) \\ 0 & 1 & 0 & 0 \\ 0 & 0 & 0 & 1 \end{bmatrix}$$

$$^3T_4 = \begin{bmatrix} cos(0) & 0 & sin(0) & 0 \\ sin(0) & 0 & -cos(0) & 0 \\ 0 & 1 & 0 & -1592.5 \\ 0 & 0 & 0 & 1 \end{bmatrix}$$

$$
{}^{4}T_{5} = \begin{bmatrix} cos\left(-\frac{\pi}{2}\right) & 0 & sin\left(-\frac{\pi}{2}\right) & 0 \\ sin\left(-\frac{\pi}{2}\right) & 0 & -cos\left(-\frac{\pi}{2}\right) & 0 \\ 0 & 1 & 0 & 0 \\ 0 & 0 & 0 & 1 \end{bmatrix}
$$

$$
{}^{5}T_{6} = \begin{bmatrix} cos(0) & -sin(0) & 0 & 0 \\ sin(0) & cos(0) & 0 & 0 \\ 0 & 0 & 1 & 200 \\ 0 & 0 & 0 & 1 \end{bmatrix}
$$

Multiplying all homogeneous transformations matrix, we have the following:

$$
{}^{0}T_{6} = {}^{0}T_{1}\,{}^{1}T_{2}\,{}^{2}T_{3}\,{}^{3}T_{4}\,{}^{4}T_{5}\,{}^{5}T_{6} = \begin{bmatrix} 0.707 & -0.707 & 0 & 770.557 \\ -0.707 & -0.707 & 0 & -770.557 \\ 0 & 0 & -1 & 1760.537 \\ 0 & 0 & 0 & 1 \end{bmatrix}
$$

So the position of point P is $P = \left[770.557 \quad \text{-}770.557 \quad 1760.537\right]^{T}$ (mm)

3. Inverse kinematic

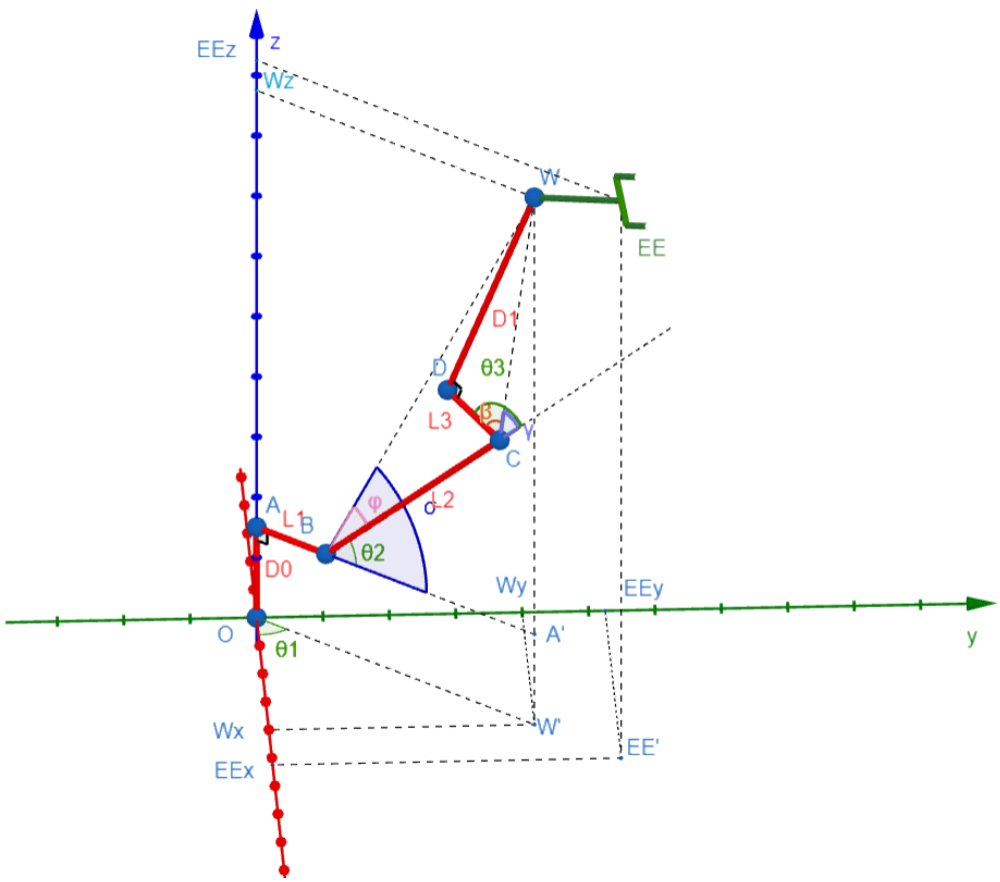

To calculate the end effector coordinate (work point) in the coordinate system, we need to separate this problem into two separate problems, end effector orientation and wrist position.

Wrist position: From the coordinate of end effector and orientation of ${}^{0}R_{6}$, we can find the position of wrist (Spherical Wrist)

$$ {}^{0}r_{6} = {}^{0}R_{6}{}^{6}r + {}^{6}d $$

$$ \begin{bmatrix} W_X \\ W_Y \\ W_Z \end{bmatrix} = \begin{bmatrix} X \\ Y \\ Z \end{bmatrix} - {}^{0}R_{6} \begin{bmatrix} 0 \\ 0 \\ 200 \end{bmatrix} $$

At this point, the problem becomes an inverse kinematics of a 3 DOF robot, simplifying the problem. From this point we can calculate θ_1, θ_2 and θ_3

End effector orientation: From the orientation matrix ${}^0R_6$ and the values of θ_1, θ_2 and θ_3, we can determine the matrix ${}^0R_3$. From the 3 matrices ${}^0R_6$, ${}^0R_3$ and ${}^3R_6$, we can calculate the values of θ_4 ,θ_5 and θ_6

3.1 Method and analysis of inverse kinematics

<u>Inverse kinematic of wrist position</u>:

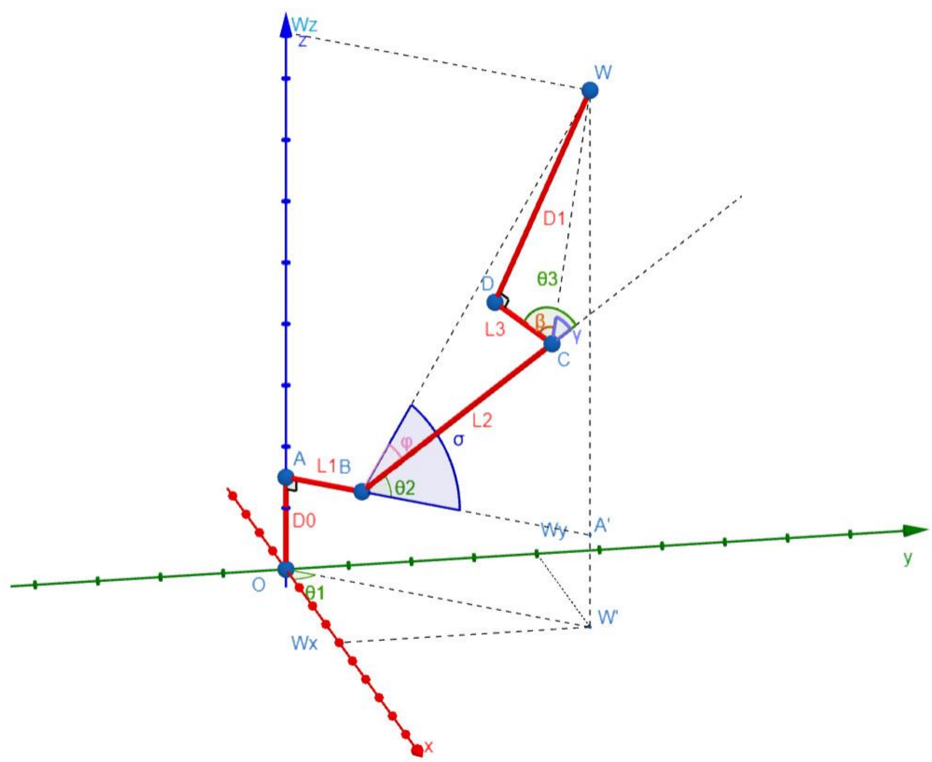

Given the robot arm's DH (Denavit-Hartenberg) parameters, we set the following lengths based on the diagram:

$$AO = D_0,\ AB = L_1,\ BC = L_2,\ DC = L_3,\ DW = D_1$$

Evaluate $\Delta OW_XW'$: $\theta_1 = atan2\left(W_XW', W_X\right) = atan2\left(W_Y, W_X\right)$

We can see that: $\theta_2 = \sigma - \varphi$

Consider $\Delta WBA'$: $\sigma = atan2(A'W, A'B)$

Employing the cosine law for triangle ΔBCW:

$$CW^2 = BW^2 + CB^2 - 2BW.CB.cos\left(WBC\right)$$

Where as: $CW^2 = L_3^2 + D_1^2$, $BW^2 = \left(\sqrt{W_X^{\ 2} + W_Y^{\ 2}} - \mathrm{L}_1\right)^2 + \left(W_Z - D_0\right)^2$, $CB^2 = L_2^2$

$$\Leftrightarrow cos\left(WBC\right) = \frac{\left(\sqrt{W_X^{\ 2} + W_Y^{\ 2}} - \mathrm{L}_1\right)^2 + \left(W_Z - D_0\right)^2 + L_2^{\ 2} - \left(L_3^{\ 2} + D_1^{\ 2}\right)}{2.\sqrt{\left(\sqrt{W_X^{\ 2} + W_Y^{\ 2}} - \mathrm{L}_1\right)^2 + \left(W_Z - D_0\right)^2}.L_2} = cos\left(\varphi\right) \quad (1)$$

We also have: $sin^2\left(\varphi\right) + cos^2\left(\varphi\right) = 1 \Leftrightarrow sin\left(\varphi\right) = \pm\sqrt{1 - cos^2\left(\varphi\right)}$ (2)

From (1) and (2): $\varphi = atan2(sin\varphi, cos\varphi)$

Therefore θ_2 will in two angles:

$$\begin{aligned}\theta_2 &= \sigma - \varphi = atan2\left(A'W, A'B\right) - atan2\left(sin\varphi, cos\varphi\right) \\ &= atan2\left(W_Z - D_0, \sqrt{W_X^{\ 2} + W_Y^{\ 2}} - L_1\right) - atan2\left(\pm\sqrt{1 - cos^2(\varphi)}, cos\varphi\right)\end{aligned}$$

We also have: $\theta_3 = \beta + \gamma$

Consider right triangle ΔDCW, we have:

$$\beta = atan2\left(D_1, L_3\right)$$

Consider ΔBCW, we have:

$$BW^2 = CW^2 + CB^2 - 2CW.CB.cos\left(BCW\right)$$

$$\Leftrightarrow cos\left(BCW\right)=\frac{L_3^{\,2}+D_1^{\,2}+L_2^{\,2}-\left[\left(\sqrt{W_X^{\,2}+W_Y^{\,2}}-\mathrm{L}_1\right)^2+\left(W_Z-D_0\right)^2\right]}{2.\sqrt{L_3^{\,2}+D_1^{\,2}}.L_2}$$

However: $cos\left(BCW\right)=cos\left(\pi-\gamma\right)=-cos\left(\gamma\right)$

$$\Leftrightarrow cos\left(\gamma\right)=-\frac{L_3^{\,2}+D_1^{\,2}+L_2^{\,2}-\left[\left(\sqrt{W_X^{\,2}+W_Y^{\,2}}-\mathrm{L}_1\right)^2+\left(W_Z-D_0\right)^2\right]}{2.\sqrt{L_3^{\,2}+D_1^{\,2}}.L_2}$$

We also have: $sin^2\left(\gamma\right)+cos^2\left(\gamma\right)=1\Leftrightarrow sin\left(\gamma\right)=\pm\sqrt{1-cos^2\left(\gamma\right)}$

$$\Rightarrow \gamma = atan2\left(\pm\sqrt{1-cos^2\left(\gamma\right)},cos\left(\gamma\right)\right)$$

Therefore θ_3 will also have two angles:

$$\theta_3 = atan2\left(D_1,L_3\right)+atan2\left(\pm\sqrt{1-cos^2\left(\gamma\right)},cos\left(\gamma\right)\right)$$

Ultimately, we will have $1\,\theta_1$, $2\,\theta_2$, $2\,\theta_3$. If we permutate all these angles, we will get 4 different sets of possible angles. However, θ_1 can also have 2 angles, resulting in 8 different sets of angles.

Inverse kinematic – Orientation:

To derive the orientation part of inverse kinematics, we begin with the transformation matrix T from the base to the end effector, represented as:

$${}^0T_3=\begin{bmatrix} c\theta_1 c(\theta_2-\theta_3) & -s\theta_1 & -s(\theta_2-\theta_3)c\theta_1 & 40c\theta_1[5c(\theta_2-\theta_3)+32c\theta_2+8] \\ s\theta_1 c(\theta_2-\theta_3) & c\theta_1 & -s(\theta_2-\theta_3)s\theta_1 & 40s\theta_1[5c(\theta_2-\theta_3)+32c\theta_2+8] \\ s(\theta_2-\theta_3) & 0 & c(\theta_2-\theta_3) & 200s(\theta_2-\theta_3)+1280s\theta_2+780 \\ 0 & 0 & 0 & 1 \end{bmatrix}$$

$$\rightarrow {}^0R_3=\begin{bmatrix} c(\theta_2-\theta_3)c\theta_1 & -s\theta_1 & -s(\theta_2-\theta_3)c\theta_1 \\ c(\theta_2-\theta_3)s\theta_1 & c\theta_1 & -s(\theta_2-\theta_3)s\theta_1 \\ s(\theta_2-\theta_3) & 0 & c(\theta_2-\theta_3) \end{bmatrix}$$

The overall orientation ${}^{0}R_{6}$ from the base to the end effector can be obtained from the total transformation ${}^{0}T_{6}$, where ${}^{0}R_{6}$ is a part of ${}^{0}T_{6}$ in the form:

$$ {}^{0}R_{6} = \begin{bmatrix} r_{11} & r_{12} & r_{13} \\ r_{21} & r_{22} & r_{23} \\ r_{31} & r_{32} & r_{33} \end{bmatrix} $$

The relationship between the orientation at the third joint and the end effector is given by the equation:

$$ {}^{0}R_{6} = {}^{0}R_{3}\,{}^{3}R_{6} $$

To find ${}^{3}R_{6}$,we rearrange the equation to get:

$$ {}^{3}R_{6} = {}^{0}R_{3}^{-1}\ {}^{0}R_{6} $$

$$ \rightarrow {}^{3}R_{6} = \begin{bmatrix} c(\theta_2-\theta_3)c\theta_1 & -s\theta_1 & -s(\theta_2-\theta_3)c\theta_1 \\ c(\theta_2-\theta_3)s\theta_1 & c\theta_1 & -s(\theta_2-\theta_3)s\theta_1 \\ s(\theta_2-\theta_3) & 0 & c(\theta_2-\theta_3) \end{bmatrix}^{-1} \begin{bmatrix} r_{11} & r_{12} & r_{13} \\ r_{21} & r_{22} & r_{23} \\ r_{31} & r_{32} & r_{33} \end{bmatrix} = \begin{bmatrix} s_{11} & s_{12} & s_{13} \\ s_{21} & s_{22} & s_{23} \\ s_{31} & s_{32} & s_{33} \end{bmatrix} $$

However, ${}^{3}R_{6}$ also has a form:

$$ \rightarrow {}^{3}R_{6} = \begin{bmatrix} s\theta_4 s\theta_6 + c\theta_4 c\theta_5 c\theta_6 & s\theta_4 c\theta_6 - c\theta_4 c\theta_5 s\theta_6 & c\theta_4 s\theta_5 \\ -c\theta_4 s\theta_6 + s\theta_4 c\theta_5 c\theta_6 & -c\theta_4 c\theta_6 - s\theta_4 c\theta_5 s\theta_6 & s\theta_4 s\theta_5 \\ s\theta_5 c\theta_6 & -s\theta_5 s\theta_6 & -c\theta_5 \end{bmatrix} $$

We can conclude that:

$$ \begin{bmatrix} s_{11} & s_{12} & s_{13} \\ s_{21} & s_{22} & s_{23} \\ s_{31} & s_{32} & s_{33} \end{bmatrix} = \begin{bmatrix} s\theta_4 s\theta_6 + c\theta_4 c\theta_5 c\theta_6 & s\theta_4 c\theta_6 - c\theta_4 c\theta_5 s\theta_6 & c\theta_4 s\theta_5 \\ -c\theta_4 s\theta_6 + s\theta_4 c\theta_5 c\theta_6 & -c\theta_4 c\theta_6 - s\theta_4 c\theta_5 s\theta_6 & s\theta_4 s\theta_5 \\ s\theta_5 c\theta_6 & -s\theta_5 s\theta_6 & -c\theta_5 \end{bmatrix} $$

Once ${}^{3}R_6$ is known, we can solve for the joint angles θ_4, θ_5, and θ_6 using the following equations derived from the matrix analysis:

$$\theta_4 = atan2(s_{23}, s_{13})$$

$$\theta_5 = atan2(\sqrt{s_{13}{}^2 + s_{23}{}^2}, -s_{33})$$

$$\theta_6 = atan2(-s_{32}, s_{31})$$

3.2 Results

From those solved equations, we can get that:

$$\theta_1 = a\tan 2\left(W_X W', W_X\right) = a\tan 2\left(W_Y, W_X\right)$$

$$\theta_2 = \sigma - \varphi = atan2\left(W_Z - D_0, \sqrt{W_X{}^2 + W_Y{}^2} - L_1\right) - atan2\left(\pm\sqrt{1 - cos^2(\varphi)}, cos\varphi\right)$$

$$\theta_3 = atan2\left(D_1, L_3\right) + atan2\left(\pm\sqrt{1 - \cos^2(\gamma)}, \cos(\gamma)\right)$$

$$\theta_4 = atan2\left(s_{23}, s_{13}\right)$$

$$\theta_5 = atan2\left(\sqrt{s_{13}{}^2 + s_{23}{}^2}, -s_{33}\right)$$

$$\theta_6 = atan2\left(-s_{32}, s_{31}\right)$$

3.3 Example

Let the end effector position of IRB 6700 be at $P_0 = \begin{bmatrix}1000 & 1000 & 2000\end{bmatrix}^T$ (mm) with the end effector orientation be ${}^{6}R_0 = \begin{bmatrix} 0 & 0 & 1 \\ 0 & -1 & 0 \\ 1 & 0 & 0 \end{bmatrix}$, the given dimension are $D_0 = 780$, $D_1 = 1592.5$, $L_1 = 320$, $L_2 = 1280$, $L_3 = 200$. Find the angle that best corresponds to the given position and orientation.

We will first calculate the wrist position based on this equation:

$$\begin{bmatrix} W_X \\ W_Y \\ W_Z \end{bmatrix} = \begin{bmatrix} P_X \\ P_Y \\ P_Z \end{bmatrix} - {}^0R_6 \begin{bmatrix} 0 \\ 0 \\ 200 \end{bmatrix}$$

With which $\begin{bmatrix} P_X & P_Y & P_Z \end{bmatrix}^T = \begin{bmatrix} 1000 & 1000 & 2000 \end{bmatrix}^T$ and ${}^6R_0 = \begin{bmatrix} 0 & 0 & 1 \\ 0 & -1 & 0 \\ 1 & 0 & 0 \end{bmatrix}$

$$\Leftrightarrow \begin{bmatrix} W_X \\ W_Y \\ W_Z \end{bmatrix} = \begin{bmatrix} 1000 \\ 1000 \\ 2000 \end{bmatrix} - \begin{bmatrix} 0 & 0 & 1 \\ 0 & -1 & 0 \\ 1 & 0 & 0 \end{bmatrix} \begin{bmatrix} 0 \\ 0 \\ 200 \end{bmatrix} = \begin{bmatrix} 800 \\ 1000 \\ 2000 \end{bmatrix}$$

Using the calculated wrist position:

We first calculate θ_1:

$$\theta_1 = atan2(W_Y, W_X) = atan2(1000{,}800) \approx 0.8961(rad) = 51.3402^{o}$$

Then we calculate θ_2:

$$cos(\varphi) = \frac{\left(\sqrt{W_X{}^2 + W_Y{}^2} - \mathrm{L}_1\right)^2 + (W_Z - D_0)^2 + L_2{}^2 - \left(L_3{}^2 + D_1{}^2\right)}{2.\sqrt{\left(\sqrt{W_X{}^2 + W_Y{}^2} - \mathrm{L}_1\right)^2 + (W_Z - D_0)^2}.L_2}$$

$$= \frac{\left(\sqrt{800^2 + 1000^2} - 320\right)^2 + (2000 - 780)^2 + 1280^2 - \left(200^2 + 1592.5^2\right)}{2.\sqrt{\left(\sqrt{800^2 + 1000^2} - 320\right)^2 + (2000 - 780)^2}.1280} \approx 0.3707$$

$$\Rightarrow sin(\varphi) = \pm\sqrt{1 - cos^2(\varphi)} = \pm\sqrt{1 - 0.3707^2} = \pm 0.9288$$

We get two θ_2:

$$\theta_{2(1)} = atan2\left(W_Z - D_0, \sqrt{W_X{}^2 + W_Y{}^2} - L_1\right) - atan2\left(\sqrt{1 - cos^2(\varphi)}, cos\varphi\right)$$

$$= atan2\left(2000 - 780, \sqrt{800^2 + 1000^2} - 320\right) - atan2(0.9287, 0.3706)$$

$$\approx -0.29(rad) = -16.46^{o}$$

$$\theta_{2(2)} = atan2\left(W_Z - D_0, \sqrt{W_X{}^2 + W_Y{}^2} - L_1\right) - atan2\left(-\sqrt{1 - cos^2(\varphi)}, cos\varphi\right)$$

$$= atan2\left(2000 - 780, \sqrt{800^2 + 1000^2} - 320\right) - atan2(-0.9287, 0.3706)$$

$$\approx 2.09(rad) = 120.02^{\mathrm{o}}$$

However, in the simulation, the actual value of θ_2 is $\theta_{2_{sim}} = -\theta_2 + \frac{\pi}{2}$ due to the fact that at zero position, the initial value of $\theta_{2_{sim}}$ is offset by $\frac{\pi}{2}$ and it rotates in the reverse direction with respect to the positive rotation given by the dataset

And finally, we calculate θ_3:

$$cos(\gamma) = -\frac{L_3{}^2 + D_1{}^2 + L_2{}^2 - \left[\left(\sqrt{W_X{}^2 + W_Y{}^2} - \mathrm{L}_1\right)^2 + \left(W_Z - D_0\right)^2\right]}{2.\sqrt{L_3{}^2 + D_1{}^2}.L_2}$$

$$= -\frac{200^2 + 1592.5^2 + 1280^2 - \left[\left(\sqrt{800^2 + 1000^2} - 320\right)^2 + \left(2000 - 780\right)^2\right]}{2.\sqrt{200^2 + 1592.5^2}.1280} \approx -0.4389$$

$$\Rightarrow sin(\gamma) = \pm\sqrt{1 - cos^2(\gamma)} = \pm\sqrt{1 - (-0.4389)^2} = \pm 0.8985$$

We also get two θ_3:

$$\theta_{3(1)} = atan2(D_1, L_3) + atan2\left(\sqrt{1 - cos^2(\gamma)}, cos(\gamma)\right)$$

$$= atan2(1592.5, 200) + atan2(0.8985, -0.4389)$$

$$\approx -3.4710(rad) = \text{-}198.8738^{\mathrm{o}}$$

$$\theta_{3(1)} = atan2(D_1, L_3) + atan2\left(-\sqrt{1 - cos^2(\gamma)}, cos(\gamma)\right)$$

$$= atan2(1592.5, 200) + atan2(-0.8985, -0.4389)$$

$$\approx 0.5793(rad) = 33.1903^{\mathrm{o}}$$

As stated in the *Method and analysis of inverse kinematics* section, we will get 4 different sets robot angles, however, we will choose 1 set of $\theta_1, \theta_2, \theta_3$ to demonstrate the calculation $\theta_4, \theta_5, \theta_6$.

We use $\theta_1 = 0.8961; \theta_2 = -0.29, \theta_3 = 0.5793$ to keep calculating $\theta_4, \theta_5, \theta_6$.

Then we calculate ${}^3R_6$ using inverse orientation:

$$
{}^3R_6 = \begin{bmatrix} 0.9985 & -0.0431 & 0.0345 \\ 0.0000 & -0.6247 & -0.7809 \\ 0.0552 & 0.7797 & -0.6237 \end{bmatrix}
$$

$$
= \begin{bmatrix} s\theta_4 s\theta_6 + c\theta_4 c\theta_5 c\theta_6 & s\theta_4 c\theta_6 - c\theta_4 c\theta_5 s\theta_6 & c\theta_4 s\theta_5 \\ -c\theta_4 s\theta_6 + s\theta_4 c\theta_5 c\theta_6 & -c\theta_4 c\theta_6 - s\theta_4 c\theta_5 s\theta_6 & s\theta_4 s\theta_5 \\ s\theta_5 c\theta_6 & -s\theta_5 s\theta_6 & -c\theta_5 \end{bmatrix}
$$

Therefore:

$$\theta_4 = atan2\left(s_{23}, s_{13}\right) \approx -1.5266\left(rad\right) = -87.4709^{\circ}$$

$$\theta_5 = atan2\left(\sqrt{s_{13}{}^2 + s_{23}{}^2}, -s_{33}\right) \approx 0.8973\left(rad\right) = 51.4101^{\circ}$$

$$\theta_6 = atan2\left(-s_{32}, s_{31}\right) \approx -1.5001\left(rad\right) = -85.9494^{\circ}$$

However, in the simulation, the actual value of θ_5 is $\theta_{5_{sim}} = -\theta_5$ since it rotates in the reverse direction with respect to the positive rotation given by the dataset.

III. SIMULATION

1. Simulation results

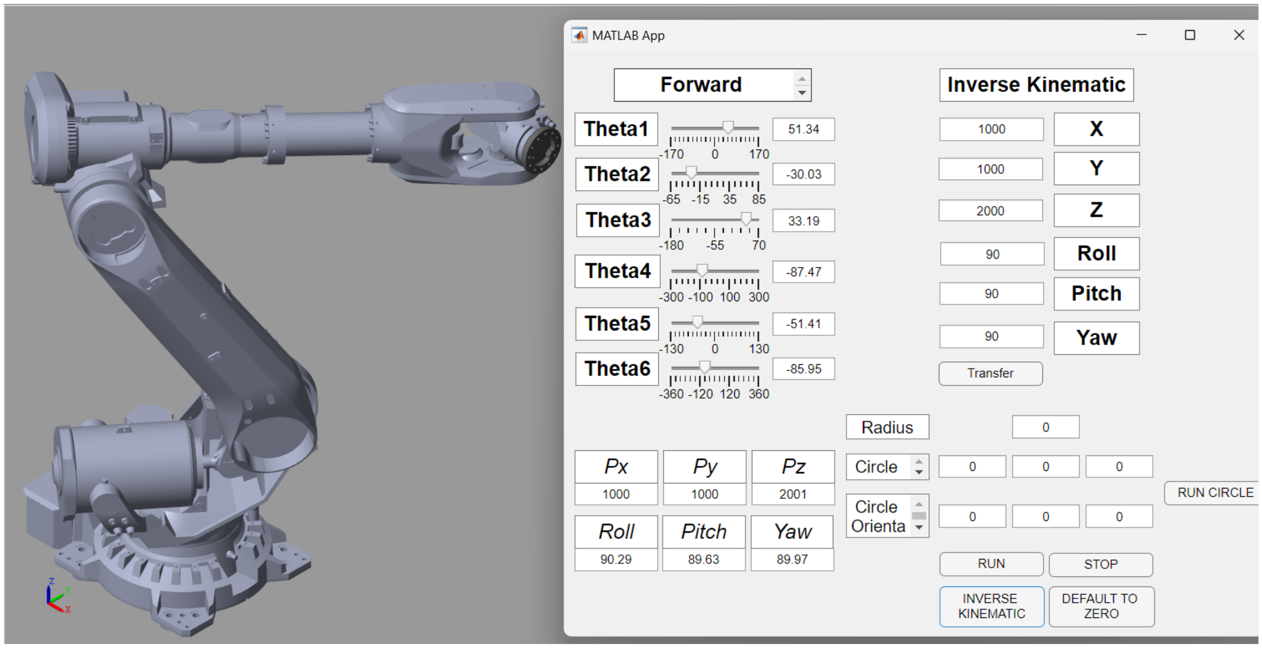

2. Code simulation

Because in matlab doesn't have symbol

2.1 Forward kinematic

```
function result = ForwardKinematic(app)
      theta1 = app.Theta1_Slider.Value * pi / 180;
      theta2 = app.Theta2_Slider.Value * pi / 180;
      theta3 = app.Theta3_Slider.Value * pi / 180;
      theta4 = app.Theta4_Slider.Value * pi / 180;
      theta5 = app.Theta5_Slider.Value * pi / 180;
      theta6 = app.Theta6_Slider.Value * pi / 180;
T1 = [[cos(theta1)      0       -sin(theta1)     320 * cos(theta1) ]
      [sin(theta1)      0       cos(theta1)      320 * sin(theta1) ]
      [0                -1      0                780               ]
      [0                0       0                1                 ]];
T2 = [[cos(theta2)      -sin(theta2)    0        1280 * cos(theta2)]
```

```
      [sin(theta2)      cos(theta2)     0       1280 * sin(theta2)]
      [0                0               1       0                 ]
      [0                0               0       1                 ]];
T3 = [[cos(theta3)      0       -sin(theta3)    200 * cos(theta3) ]
      [sin(theta3)      0       cos(theta3)     200 * sin(theta3) ]
      [0                -1      0               0                 ]
      [0                0       0               1                 ]];
T4 = [[cos(theta4)      0       sin(theta4)     0                 ]
      [sin(theta4)      0       -cos(theta4)    0                 ]
      [0                1       0               1592.5            ]
      [0                0       0               1                 ]];
T5 = [[cos(theta5)      0       -sin(theta5)    0                 ]
      [sin(theta5)      0       cos(theta5)     0                 ]
      [0                -1      0               0                 ]
      [0                0       0               1                 ]];
T6 = [[cos(theta6)      -sin(theta6)    0       0                 ]
      [sin(theta6)      cos(theta6)     0       0                 ]
      [0                0               1       200               ]
      [0                0               0       1                 ]];
T06 = T1 * T2 * T3 * T4 * T5 * T6;
fixError = zeros(size(T06));
fixError(abs(T06) > 1e-6) = 1;
T06 = T06 .* fixError;
pos =  T06 * [0; 0; 0; 1];
app.ForwardPx.Value = pos(1, 1);
app.ForwardPy.Value = pos(2, 1);
app.ForwardPz.Value = pos(3, 1);
theta = atan2(sqrt(T06(3, 1) ^ 2 + T06(3, 2) ^ 2), T06(3,3));
psi = atan2(T06(1, 3), T06(2, 3));
phi = atan2(T06(3, 1), -T06(3, 2));
app.RollDisp.Value = phi;
```

```
app.PitchDisp.Value = theta;

app.YawDisp.Value = psi;

result = {pos, phi, theta, psi};

end
```

2.2 Inverse kinematic

```
function InverseKinematic(app, Xtarget, Ytarget, Ztarget, phi, theta, psi)

% Create Roll - Pitch - Yaw Rotation matrix

R06 = [cos(phi) * cos(psi) - cos(theta) * sin(phi) * sin(psi),      sin(phi)
* cos(psi) + cos(theta) * cos(phi) * sin(psi),      sin(theta) * sin(psi);

-cos(phi) * sin(psi) - cos(theta) * sin(phi) * cos(psi),     -sin(phi) *
sin(psi) + cos(theta) * cos(phi) * cos(psi),     sin(theta) * cos(psi);

sin(theta) * sin(phi),                                       -cos(phi) *
sin(theta),                                      cos(theta)           ];

% Fix the issue where zero are calculated as -0.00000,

% potentially throwing off the calculation

fixError = zeros(size(R06));

fixError(abs(R06) > 1e-6) = 1;

R06 = R06 .* fixError;

% Calculate wrist position

XYZtarget = [Xtarget Ytarget Ztarget]' - R06 * [0 0 200]';

X = XYZtarget(1); Y = XYZtarget(2); Z = XYZtarget(3);

% Calculate first angle

theta1_val = atan2(Y, X);

% Initialize the dimension of robot arm from base to wrist

% according the geogebra diagram

D0 = 780;

L1 = 320;

L2 = 1280;

L3 = 200;

D1 = 1592.5;
```

```
% Calculation of theta2, theta3 according to our report
beta = atan2(D1, L3);
sigma = atan2(Z - D0, sqrt(X^2 + Y^2) - L1);
BW = sqrt((Z - D0) ^ 2 + (sqrt(X^2 + Y^2) - L1) ^ 2);
CB = L2;
CW = sqrt(L3^2 + D1^2);
cosphi = (BW^2 + CB^2 - CW^2) / (2 * BW * CB);
phi1 = atan2(sqrt(1 - cosphi^2), cosphi);
phi2 = atan2(-sqrt(1 - cosphi^2), cosphi);
% This will results 2 theta2
theta2_val1 = sigma - phi1;
theta2_val2 = sigma - phi2;
cosgamma = -(CB^2 + CW^2 - BW^2) / (2 * CB * CW);
gamma1 = atan2(sqrt(1 - cosgamma^2), cosgamma);
gamma2 = atan2(-sqrt(1 - cosgamma^2), cosgamma);
% And 2 theta3
theta3_val1 = -(gamma1 + beta);
theta3_val2 = -(gamma2 + beta);
positionAngles = [theta1_val theta2_val1 theta3_val1;
theta1_val theta2_val2 theta3_val2];
sliderFields = {app.Theta1_Slider, app.Theta2_Slider, app.Theta3_Slider, ...
app.Theta4_Slider, app.Theta5_Slider, app.Theta6_Slider};
possibleAngles = app.EERotation(positionAngles, R06);
values = [];
syms theta1 theta2 theta3 theta4 theta5 theta6
angleConverter = [rad2deg(theta1) rad2deg(-(theta2 - pi/2)) rad2deg(theta3)
rad2deg(theta4) rad2deg(-theta5) rad2deg(theta6)];
varName = [theta1 theta2 theta3 theta4 theta5 theta6];
for i = 1: length(possibleAngles)
      for j = 1:6
```

```
          convertedAngle = double(subs(angleConverter(j), varName(j), possibleAngles{i}(j)));

          if convertedAngle < sliderFields{j}.Limits(2) && convertedAngle > sliderFields{j}.Limits(1)

              values = [values, convertedAngle];

          end

      end

      if length(values) == 6

          break

      else

          values = [];

      end

end

if length(values) < 6

      error('No configuration is found', "The coordinates input is out of range for IRB 6700");

end

numericFields = {app.Theta1_Field, app.Theta2_Field, app.Theta3_Field, ...

app.Theta4_Field, app.Theta5_Field, app.Theta6_Field};

% Gradual slider control

app.MultipleGUIControl(sliderFields, numericFields, values);

end
```

CONCLUSION

Robots are playing an increasingly important role in our lives, from industrial manufacturing to customer service and various other fields. Advances in artificial intelligence and robotics have brought about significant potential for societal development. However, to ensure that robots not only generate economic benefits but also do not have negative impacts on human jobs and lives, careful consideration and management are needed.

Understanding the concepts of forward and inverse kinematics, as well as simulation from reports, is crucial in grasping the essence of robots, especially in the industrial sector. Forward kinematics involves programming robots to perform tasks accurately and efficiently, while inverse kinematics focuses on improving outcomes based on feedback from the environment.

Simulation from reports is an essential tool for reproducing virtual environments, enabling researchers and developers to test and evaluate control methods and robot programming effectively.

Overall, a clear understanding of these concepts not only helps us comprehend how robots operate in industry but also aids in developing and applying this technology intelligently and efficiently across various industrial sectors.